Non-Native Interhelical Hydrogen Bonds in the Cystic Fibrosis Transmembrane Conductance Regulator Domain Modulated by Polar Mutations†

Mei Y. Choi, Lia Cardarelli, Alex G. Therien,‡ and Charles M. Deber*

Division of Structural Biology and Biochemistry, Research Institute, Hospital for Sick Children, Toronto, Ontario M5G 1X8, and Department of Biochemistry, University of Toronto, Toronto, Ontario M5S 1A8, Canada

Received March 19, 2004; Revised Manuscript Received April 27, 2004

ABSTRACT: Polar residues comprise about 15% of the transmembrane (TM) domains of proteins, where they can stabilize structure via native side chain−side chain interhelical hydrogen bonds between TM helices. However, non-native H-bonds may be implicated in disease states, through limiting protein dynamics during transport and/or misfolding the protein by inducing non-native rotational positions about TM helical axes. Here we have undertaken an investigation of the presence and strength of H-bond interactions within a series of helix−loop−helix ("hairpin") constructs derived from TM helices 3 and 4 (italic) of the cystic fibrosis transmembrane conductance regulator (CFTR) (prototypic sequence G^{194}*LALAHFVWIAPLQ*^{207}*VALLMGLI*WELLQ*ASAFAGLGFLIV*^{232}*LALFQ*^{237}*AGLG*^{241}) in which wild-type Q207 in TM3 forms an interhelical H-bond with CF-phenotypic mutant V232D in TM4 [Therien, A. G., Grant, F. E., and Deber, C. M. (2001) *Nat. Struct. Biol 8*, 597−601]. In the present work, a library of 21 TM3/4 constructs was prepared, where Asp residues were placed individually at TM4 positions 221−241. Using gel shift assays—in which H-bond-linked hairpins (closed conformation) migrate faster than the elongated forms (open conformation)—we found that Q207 in TM3 is able to "capture" all 21 TM4 D mutations into measurable populations of interhelical H-bonds. A similar library of TM4 D mutants—but also containing Q207L—reverted to wild-type migration rates, confirming Q207 as the polar partner for TM4 D residues. In view of the broad capture range of Q207, these results emphasize the potential consequences to folding and dynamics of introducing polar mutations into the TM domains of membrane proteins in the vicinity of a native polar TM residue.

Polar residues in the transmembrane (TM)[1] α-helices of membrane proteins can influence the folding or association of membrane proteins (*1*−*3*). While polar residues (including Cys, Trp, Ser, Thr, Asn, Gln, Tyr, Lys, Arg, His, Asp, and Glu residues) comprise only about 15% of the total residues native to TM domains of proteins (*4*), when they do occur, they may act to stabilize the local protein tertiary structure through the formation of side chain−side chain interhelical hydrogen bonds within the membrane environment (*5*−*7*). Indeed, approximately half of all TM helices occurring in proteins solved to high resolution display a side chain H-bond to a neighboring helix (*8*, *9*). This phenomenon takes on particular importance because patterns of phenotypic mutations occurring in the TM domains of membrane proteins linked to human disease have been found to be dominated by mutations involving gain or loss of polar residues (*10*, *11*). Such non-native electrostatic links between TM helices can be inferred to be implicated in limiting protein dynamics during transport and/or in misfolding the protein by inducing non-native rotational positions about TM helical axes.

One protein widely studied in this context is the cystic fibrosis transmembrane conductance regulator (CFTR) (*12*), in which defects are found to cause cystic fibrosis (CF). CF is the most common lethal autosomal recessive genetic disease in the Caucasian population, affecting one in two thousand births (*12*−*15*). CF mainly affects the lung and digestive system in patients, producing an imbalance of sodium and chloride ions. CFTR forms a chloride channel which is an essential component of epithelial chloride transport systems in lungs, pancreas, and sweat glands (*15*−*20*). The protein contains 1480 amino acids arranged into two largely homologous halves (*13*). Each half has a predicted six-helix-spanning transmembrane (TM) domain and a nucleotide-binding domain; a cytoplasmic regulatory (R) domain links the two halves. Although the majority of CF patients are affected by a deletion of Phe508 in the first nucleotide-binding domain, over 100 CF-phenotypic CFTR mutations occur within the TM domains (*21*). It was further noted that many of the TM-based mutations in CFTR involve

† This work was supported, in part, by grants to C.M.D. from the Canadian Cystic Fibrosis Foundation (CCFF) and the Canadian Institutes of Health Research (CIHR). M.Y.C. is grateful for an award from the Hospital for Sick Children Research Training Committee. L.C. was a student research participant in the Samuel B. Lunenfeld Summer Student Research Program. A.G.T. held a CIHR postdoctoral fellowship award.

* To whom correspondence should be addressed at the Hospital for Sick Children. E-mail: deber@sickkids.ca. Phone: (416) 813-5924. Fax: (416) 813-5005.

‡ Present address: Merck Frosst Canada & Co., P.O. Box 1005, Pointe-Claire, Quebec H9R 4P8, Canada.

[1] Abbreviations: CF, cystic fibrosis; CFTR, cystic fibrosis transmembrane conductance regulator; TM, transmembrane; VD, V232D; wt, wild type; PAGE, polyacrylamide gel electrophoresis; SDS, sodium dodecyl sulfate; CD, circular dichroism; H-bond, hydrogen bond; RP-HPLC, reversed-phase high-performance liquid chromatography; LB, Luria−Bertani; MW, molecular weight; TFE, trifluoroethanol.

10.1021/bi0494525 CCC: $27.50 © 2004 American Chemical Society
Published on Web 06/05/2004

apolar-to-polar amino acid substitutions that similarly have the potential to form non-native H-bonds with a native "polar partner" in the protein (*22*).

To elucidate the molecular events for CF disease arising from TM domain mutations, we have focused on expression and structural analysis of two TM segments ("helical hairpins") as the minimal model of tertiary contacts between the TM helices in CFTR. Using this approach, specific side chain−side chain interactions between TM helices can be highlighted. For example, experimental verification of the presence of interhelical H-bonds can be obtained, in part, from migration patterns of CFTR constructs on SDS−PAGE gels, on which the more compact, H-bond-linked hairpins (closed conformation) are seen to migrate faster than the elongated forms (open conformation) whose movement is retarded (*22*, *23*). With the use of this "gel-shift assay" on SDS−PAGE, we observed that the construct derived from the phenotypic mutant Val232-Asp—which induces a mild form of CF—migrated significantly faster than the wt construct (*22*), indicating that V232D adopts a more compact conformation likely imposed by a tight interaction between the mutant Asp 232 in TM helix 4 and its polar partner Gln 207 in TM helix 3 (*22*). Using this approach in a wider context, one should accordingly be able to detect the formation and extent of non-native interactions within the TM3/4 construct for CF-phenotypic and other mutants of interest.

Formation of an H-bond through the pairing of two polar side chains between TM helices depends on both the proximity of the two side chains and the rotational freedom of the respective helices around their major axes. In the present work, we undertook investigations of the presence and strength of H-bond interactions within a series of CFTR TM3/4 constructs. Asp-scanning mutagenesis studies on CFTR TM helix 4 (using the α-helical hairpin of the CFTR TM helix 3/4 construct) was employed to determine the ability of the helix to rotate around its own axis to satisfy H-bonding interactions with a polar partner in its neighboring helix. This study also shed light on the ability of the Gln side chain (Gln 207 in TM helix 3) to "capture" the mutant Asp side chains in the neighboring helix (TM helix 4).

MATERIALS AND METHODS

Expression of the Thioredoxin-Fused TM3/4 Construct of CFTR. The cDNAs encoding the amino acids in TM3/4 (wt residues 194−241) were subcloned into the pET32a vector by procedures adapted from Therien et al. (*24*). Mutants (single-point mutations within TM4) were generated using the QuikChange site-directed mutagenesis kit (Stratagene). Target mutations were confirmed by direct DNA sequencing. Each construct was transformed into the BL21(DE3) cells. A fresh colony was grown in 10 mL of LB medium with 100 μg/mL ampicillin antibiotic with shaking (250 rpm at 37 °C) for 3 h. The culture was then diluted 1:50 with M9 medium, and growth was continued until $OD_{600} \approx 0.6$. Next, the culture was induced with 0.1 mM IPTG, and at the same time, an additional 100 μg/mL ampicillin antibiotic was added to the cultures, and the cultures were grown further overnight with shaking (250 rpm) at room temperature. The cells were harvested at 10 000*g* for 20 min in a JA10.5 rotor.

Optimization of Purification of CFTR TM3/4 Constructs. The purification procedures were adapted from Therien et al. (*24*). Each 500 mL cell pellet was lysed by sonication in 20 mM Tris buffer with 1 mg/mL lysozyme. The clear mixture was supplemented with 150 mM NaCl, 10 mM β-mercaptoethanol, and 5 mM imidazole. The soluble fraction was separated by centrifugation at 27 000 *g* for 20 min. The supernatant was then added to 10 mL of His-bound resin and allowed to bind the protein with gentle rocking overnight at room temperature. The mixture was allowed to flow through, and the resin was washed six times with 10 mL of wash buffer (150 mM NaCl, 10 mM β-mercaptoethanol, 50 mM imidazole, 0.2% Triton, 20 mM Tris−Cl, pH 8.0). The protein was eluted twice with 10 mL of 100 mM imidazole wash buffer. The eluate was then supplemented with 5 mM $CaCl_2$ and thrombin and incubated with gentle rocking at room temperature overnight for cleavage of the thioredoxin tag. The cleaved protein was purified by RP-HPLC on a C4 semipreparative column (Phenomenex) using a water/2-propanol gradient (5−95% 2-propanol over 70 min at a flow rate of 3 mL/min). The peaks were collected, confirmed by mass spectrometry, and lyophilized.

Circular Dichroism (CD) Spectroscopy Analysis. CD spectra were collected using a Jasco J-720 circular dichroism spectropolarimeter. Samples were measured at protein concentrations between 25 and 50 μM and were dissolved in 10 mM SDS and 10 mM Tris at pH 8.0. Measurements were taken using a quartz cuvette with a path length of 0.1 mm. Spectral scans were performed from 250 to 190 nm with a step resolution of 0.4 nm, a speed of 20 nm/min, and a bandwidth of 1.0 nm. The reported result was obtained from the average value of three spectral scans, and the protein concentrations were determined by amino acid analysis.

PAGE Analysis. The dry protein samples were resuspended in NuPage LDS sample buffer, and 1 μg of each protein was run on 12% NuPAGE Bis-Tris gels with MES running buffer. The gels were stained with Coomassie Blue (according to standard protocols) for analysis.

Migration Analysis of each X → D Mutant on SDS−PAGE. Each X → D mutant was run on SDS−PAGE side by side with the wt TM3/4 construct and two molecular weight (MW) markers. The percentage of apparent MW decrease for each X → D mutant in TM4 was calculated from each stained gel, by comparing the apparent molecular weight observed in the migrations (with the use of the NIH 1.62 Image Program, software available at http://www-cellbio.med.unc.edu/henson_mrm/pages/NIH.html) vs the theoretical molecular weight based on the amino acid sequence. Each value is the average ± SD of at least three separate experiments.

RESULTS

We expressed each CFTR TM3/4 helix−loop−helix construct in *E. coli* as a thioredoxin fusion protein in BL21-(DE3) cells. The final construct after the cleavage of the thioredoxin tag—which includes the S-tag and His-tag from the pET32a vector (*24*)—is shown in Figure 1. Asp-scanning mutagenesis studies were performed on the full TM4 helix (residues 221−241). The expression levels of the various mutants were generally high and comparable. The mutants were purified by Ni column chromatography; the thioredoxin tag was cleaved from the construct, followed by purification using RP-HPLC. The isolated yield for each mutant is about 5 mg/500 mL culture pellet.

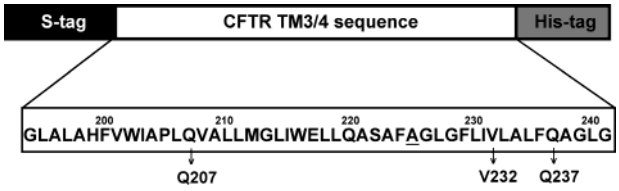

FIGURE 1: Expression of TM3/4 constructs derived from the CFTR membrane domain. Constructs were expressed as thioredoxin fusion proteins, cleaved with thrombin, and purified by HPLC (see the Materials and Methods). The final constructs used in this study correspond to residues 194−241 of CFTR TM3/4, along with an N-terminal S-tag and C-terminal His-tag. The sequence of the putative membrane-spanning regions corresponding to CFTR TM3 and TM4 is shown, with residues referred to in this study highlighted. The native Cys residue at position 225 (underlined) has been mutated to Ala to avoid complications stemming from intermolecular disulfide bonding. V232D is the original CF-phenotypic mutant studied by Therien et al. (*22*).

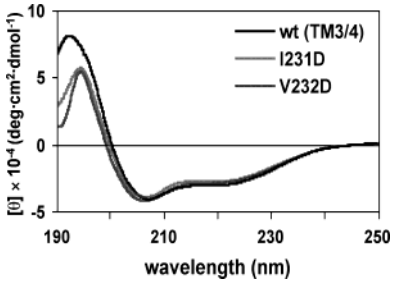

FIGURE 2: Circular dichroism spectra of selected CFTR TM3/4 constructs in sodium dodecyl sulfate (SDS) micelles. Spectra indicate essentially fully helical conformations for each construct in the micellar environment. While three spectra are shown, all D mutations examined along TM4 (221−241) displayed identical CD spectra.

Unlike most soluble proteins, the secondary structure of membrane proteins is maintained in the presence of detergents such as SDS. To confirm this observation for the present TM3/4 constructs, CD spectra were recorded for all of the designed constructs in the presence of SDS. All constructs (D221 through D241) displayed similar CD spectra, with each adopting an α-helical structure in the presence of SDS micelles with characteristic minima near 208 and 222 nm. Typical results for selected TM4 Asp mutants are shown in Figure 2. When measured against the ellipticity value observed at 222 nm of ca. −40 000° in trifluoroethanol (TFE) (spectra not shown)—a helix-promoting organic phase in which the TM3/4 constructs should be maximally helical—the ellipticity values in SDS (ca. −30 000°) (Figure 2) correspond to ca. 75% helicity, consistent with the fact that the helical hydrophobic TM3 and TM4 segments [and likely several adjacent membrane entry/exit (tag) residues] together constitute ca. two-thirds of the total 77 residues in each TM3/4 construct.

The migration rates of the TM3/4 constructs were examined on SDS−PAGE gels. Previous studies have shown that the V232D mutant migrates at a rate faster than that of the wt in NuPAGE MES gels (*22*). This migration pattern was shown to be associated with a more compact conformation of the V232D construct, imposed by a tight interaction between polar partners Asp 232 and Gln 207 of the V232D TM3/4 construct. In the present work, similar results—to varying extents—were observed for the full complement of X → D mutants along the TM4 helix (residues A221 to G241 mutated to Asp individually).

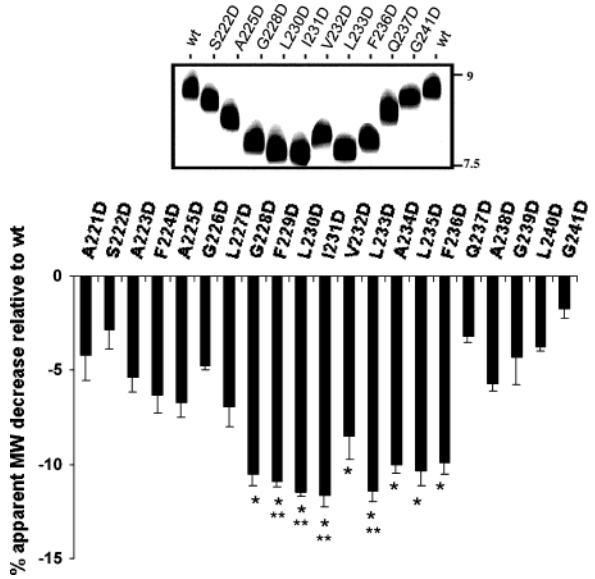

FIGURE 3: (top) Western blot analysis of selected (X → D) mutants on CFTR TM3/4 constructs. The 12% NuPAGE MES gel system is used. Varying migration rates indicate the relative populations of closed (faster migrating, strong interhelical H-bonded states) vs open (non-H-bonded states) of TM3/4 constructs. V232D is the CF-phenotypic mutant in TM4. Approximate molecular weight markers are given at the right of the diagram. (bottom) Relative apparent molecular weight percent decrease for X → D mutants in TM4. Each value was calculated by comparing the apparent molecular weight (NIH 1.62 Image Program, software available at http://www-cellbio.med.unc.edu/henson_mrm/pages/NIH.html) and the expected theoretical molecular weight, which is then subtracted from the corresponding value obtained for the wild type (6.73%). Each value is the average ± SD of at least three separate experiments. The longer downward vertical bars correspond to the stronger interhelical H-bonds. Single asterisks denote values statistically different from that of the wild type on SDS−PAGE gel ($p < 0.001$); all other constructs migrate with $p < 0.01$. Double asterisks denote values statistically different from that of the construct V232D on SDS−PAGE gel ($p < 0.01$).

Each X → D mutant in TM4 migrated faster than the wt on SDS−PAGE (12% NuPAGE MES gel system, Invitrogen). Figure 3a displays the overall gel-shift assay pattern for selected mutants along the TM4 helix. The roughly concave-shaped pattern of the Asp mutants on the SDS−PAGE gel initially distinguishes among the Asp residues of mutant TM4s that are presumed further away from Q207 (located in mid-TM3) and those that are anticipated to be directly across the hairpin vis-à-vis Q207. When these results are quantitated for the full TM4 D mutant library (Figure 3b), we find that the I231D construct has the largest negative percentage molecular weight decrease relative to the wt (−11.65% ± 0.61%), and hence migrated the furthest among all the mutants in TM4 on SDS−PAGE. Therefore, this mutant would be predicted to form the tightest H-bond with the Q207 side chain in TM3. Interestingly, mutants G228D through I231D, and L233D through F236D, have a more negative value of the percent of MW decrease relative to the wt than the CF-phenotypic mutant V232D (Figure 3b) (see the Discussion). The remaining Asp mutants toward either terminus of the TM4 helix migrated slower than the V232D construct on SDS−PAGE. Nevertheless, all of these remaining mutants are predicted to have a more compact conformation than the wt construct.

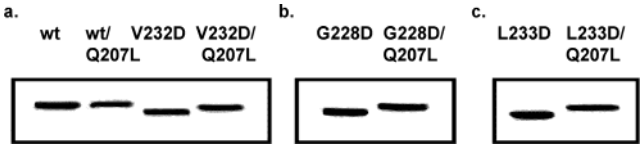

FIGURE 4: SDS−PAGE analysis for selected knockout XD/Q207L mutants. The D mutants in TM4 migrate faster than the wild-type construct, while the knockout mutants (with Q207L) retain the wt migration rate due to the fact that the polar partner in TM3 has been eliminated. Selected mutants are shown. All 21 TM4 D mutants with Q207L retained the wt migration rate.

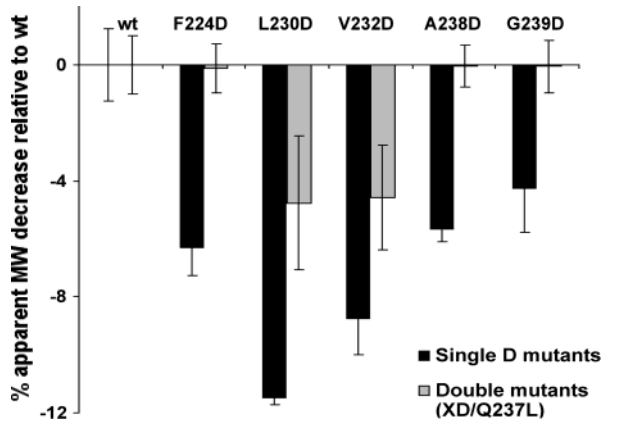

FIGURE 5: Comparison of relative migration rates on SDS−PAGE (NuPAGE MES gel system) for X → D mutants and selected XD/Q237L mutants in CFTR TM3/4 constructs. All the double mutants migrate at significantly different rates ($p < 0.01$) vs the single D mutants except the wt.

To confirm the role of Q207 as the "unique" polar partner for Asp side chains along TM4, we prepared a library of 21 TM3/4 mutants designated XD/Q207L, which has the same net charge as XD (where X is any positional D mutant in TM4) but eliminates Q207 as a possible polar partner for D mutants in TM4. These mutants were found uniformly to display the same migration rate as the wt, as shown for selected XD/Q207L constructs in Figure 4. These results are consistent with the fact that Q207 acts as the polar partner for D mutants in TM4.

Noting that CFTR TM4 also contains a native Gln residue at position 237, Partridge et al. suggested that Q237 in a CFTR single-chain TM4 peptide participates in a hydrogen bond network with residue D232 to form higher oligomers (*25*). We accordingly sought to determine whether Q237 within the TM3/4 hairpin was a stabilizing partner in addition to Q207 on (some) TM4 X → D mutants. We addressed this possibility by preparing constructs in which Q237 was mutated to Leu, while retaining Q207 and the D mutants at selected sites along the TM4 helix. Figure 5 displays the comparison of the migration differences on SDS−PAGE between six X → D mutants and their Q237L counterparts in the CFTR TM3/4 construct. Our results indicate a discrete role for Q237, viz., the double mutants F224D/Q237L, A238D/Q237L and G239D/Q237L—in which the D locus is nearer to the N- or C-terminus of the TM4 helix—returned to the wt migration rate. D mutants in mid-TM4, i.e., V232D/Q237L and L230D/Q237L, continued to migrate faster than the wt, but were clearly retarded vs their D counterparts.

DISCUSSION

In a helical hairpin construct derived from the first transmembrane domain of CFTR, the CF-phenotypic mutant V232D in TM4 was previously found to form a non-native side chain−side chain H-bond with the wild-type residue Q207 in TM3 (*22*) which was proposed to be responsible, in part, for the disruption of the functional CFTR protein. Such an interhelical H-bond "closes up" the helix−loop−helix construct, which causes the construct to migrate faster than the corresponding open structure on SDS−PAGE (*26*, *27*). This correlation between conformation and migration on SDS−PAGE was further confirmed using a TM3/4 construct with a disulfide bond at the extremities of the TM segments to constrain the construct into the closed hairpin; this construct similarly migrated at the faster rate, albeit only in the absence of a disulfide-bond-reducing reagent (*22*). Accordingly, SDS−PAGE is a valuable tool for detection of the open or closed state for a helical hairpin construct.

Asp "Walk" Mutagenesis of the CFTR TM4 Helix. All 21 X → D mutants of CFTR TM4 (residues A221 to G241 mutated to Asp individually) were expressed, and purified in milligram quantities. Evidence that these expressed fragments of CFTR membrane proteins reconstitute to a functional form was obtained from CD spectra, which established that all constructs form α-helical structures in the environment of SDS micelles (shown for selected mutants in Figure 2). We found that all Asp-containing mutants migrated faster than the wt on SDS−PAGE, indicating that each of the 21 D mutants is able to form some population of interhelical H-bonded species with the neighboring helix polar residue. To confirm that Q207 in TM3 is the (sole) polar partner in H-bond formation, a further series of 21 mutants was prepared, designated XD/QL, which has the same net charge as XD but eliminates Q207 as a possible polar partner for D mutants in TM4. This complete set of mutants reverts to the mobility displayed by the wt, establishing Q207 as likely the single polar partner for D mutants in TM4, as well as negating the argument that charge underlies the difference in migration.

Molecular Modeling Studies on the I231D Construct. The overall results suggest that H-bond formation between Asp in TM4 and Gln in TM3 underlies the difference in mobility among TM3/4 Asp mutants when compared to the wt. To verify the structural feasibility of the observations, we used a global conformation search program (GS helix program) which identifies energetically favorable packed interfaces between paired TM3/4 helices, analyzes all possible interactions between two helices defined by the user, and returns clusters of possible structures (*28*, *29*). I231D—the fastest migrating mutant—was used for the modeling studies. The paired helix model shown in Figure 6, obtained from a representative cluster, shows a tight interaction between the Gln 207 side chain carboxamide in TM3 and the Asp 231 carboxylate in TM4 (Figure 6a). An H-bond can readily form between these two side chains, with a predicted N−O distance of 2.82 Å, smaller than the average H-bond distance (3 Å) (*30*).

Our observations that interhelical H-bonds are strong determinants of helical hairpin folding can be viewed in the context of studies by Faham et al. which indicate that TM−TM packing forces are dominant over H-bonds in a series

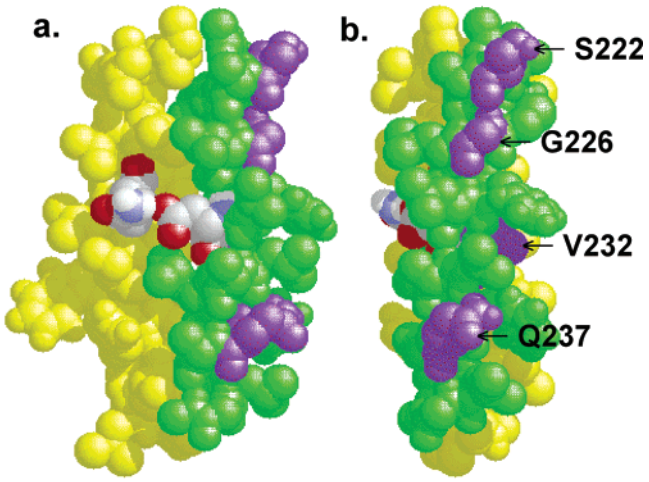

FIGURE 6: Energy-minimized structural models of antiparallel CFTR transmembrane helical segments 3 and 4 in the I231D mutant. Space-filling model of the I231D helical hairpin (intervening loop omitted). Yellow denotes TM3, green denotes TM4, and purple denotes residues at positions S222, G226, V232, and Q237 in TM4. (a) View of the I231D model showing the side chain carboxamide from Q207 in TM3 interacting with the side chain carboxylate of D231 in TM4. (b) View of the same model rotated approximately 90° to highlight the fact that residues 222, 226, 232, and 237 in TM4 are not located in interfacial positions, which may relate, in part, to the origin of the irregular "periodicity" of H-bond formation observed along TM4 (Figures 3b and 7). See the text for further discussion.

of mutants of bacteriorhodopsin (*31*). In the present CFTR systems, several factors may contribute to the importance of H-bond formation. First, as a hairpin, the CFTR TM3/4 construct may allow TM4 to rotate about its major axis to accommodate H-bond formation more readily than in TM3/4 when it occurs in the intact CFTR TM domain. As well, this rotation will inevitably produce (some) structures along the "Asp walk" wherein the native TM3/4 interface has been disrupted, and hence may lack the optimal van der Waals packing along the length of the helices. Second, similar to studies of residues that promote H-bonded dimer formation in model TM peptides (*3*, *4*), our studies involve H-bonding interactions between Gln and Asp—two of the four residues (along with Asn and Glu) that in various pairing combinations form the strongest side chain−side chain H-bonds (*3*, *4*). Pairings where at least one partner is, for example, Ser, Thr, or Tyr, may be intrinsically of somewhat lesser energy. Finally, the fact that CFTR functions as a chloride channel may impose a requirement for generally "looser" native TM−TM packing interactions to allow for protein conformational dynamics during substrate transport.

Different Migration Rates of X → D Mutants in TM4 on SDS−PAGE Gel. As displayed in Figure 3b, X → D mutants in TM4 have varying migration rates on SDS−PAGE gels. Asp mutants at positions 229−236—ostensibly those directly "across" from Q207 in the folded hairpin—migrate considerably faster than the wt construct on the SDS−PAGE gel. H-bonds in this subset of mutants may be strengthened in these cases, where both carboxamide protons of the Q207 side chain are occupied with both oxygen atoms of the Asp residue. These mutants would favor the "closed" hairpin states over the "open" hairpin states on SDS−PAGE. However, those between 221 and 227 and between 237 and 241 migrate only slightly faster than the wt construct on the SDS−PAGE gel. Although H-bond lengths to Q207 would in any case be longer in these latter instances, the results are probably most consistent with a situation where these constructs exist in mixed populations of open and closed hairpin states.

Tilting or shearing ("pulley-like") movements of one helix with respect to the other to drive H-bond formation could, in principle, contribute to the gel-shift assay effects observed. However, such structures would tend to expose hydrophobic loop and N- or C-terminal segments, and can likely be excluded since (i) the CD spectra for all the mutants [viz., the examples given in Figure 2—and for the full set of TM3/4 D221 through D241 mutants (not shown)] are superimposable and of high helicity and (ii) the loop region of this series of constructs appears de facto relatively fixed, because the strength of each H-bond is position-dependent—being the strongest at TM4 sites ostensibly best aligned to Q207—rather than equally strong in response to an "adjustable" pair of helices.

"Capture Radius" of the Glutamine Side Chain. One of the most striking results of this study is the demonstrable ability of Gln 207 in TM3 to capture essentially all TM4 D mutations into a measurable interhelical H-bond. Analysis of the side chain properties of the participant Gln and Asp residues indicates the feasibility of this situation. Thus, for example, if one assumes that I231D in TM4 forms the closest contacts with Q207 in TM3, there are 10 residues (=2.7 turns of helix) from I231D for G241D. Therefore, the vertical distance between positions 231 and 241 is about 14.6 Å (assuming one turn equals a 5.4 Å vertical displacement). For the Gln side chain in Q207, there are five bonds in total (including three C−C bonds, one C−N bond, and one N−H bond) between the main chain carbon and the side chain carboxamide group; for the Asp side chain, there are three bonds in total (including two C−C bonds and one C=O bond) between the main chain carbon and the side chain carboxylate function. Thus, the total vertical distance for the formation of an H-bond between Q207 in TM3 and G241D in TM4 will be about 15 Å (7.5 Å between the main chain carbon and the carboxamide in Q207 + 3 Å (average distance for H-bond formation) + 4.5 Å between the main chain carbon and the Asp carboxylate). Using standard side chain torsional angles, models indicate that such H-bond formation is physically realistic between Q207 in TM3 and G241D in TM4. In these latter cases, the axis of the H-bond may parallel the major helical axes of TM3/4, rather than take a more orthogonal position in H-bonds directly across from each other.

The ability of Q to capture D to form an H-bond at so many TM4 positions not only arises from bond length considerations, but is also due to the fact that the nascent helix−loop−helix construct of CFTR TM3/4 is apparently not packed tightly, which in turn enables TM4 to rotate around its own axis, bringing the required residue into the helix−helix interface, and thereby allowing H-bond formation. However, as discussed above, this apparent rotation propensity could well be considerably reduced when CFTR TM3/4 occurs in the context of the native six-TM domain of the intact protein, where interactions to additional neighboring helices must be included. The present model TM3/4 systems also assume that sequentially consecutive helices will be adjacent and aligned in the native protein—

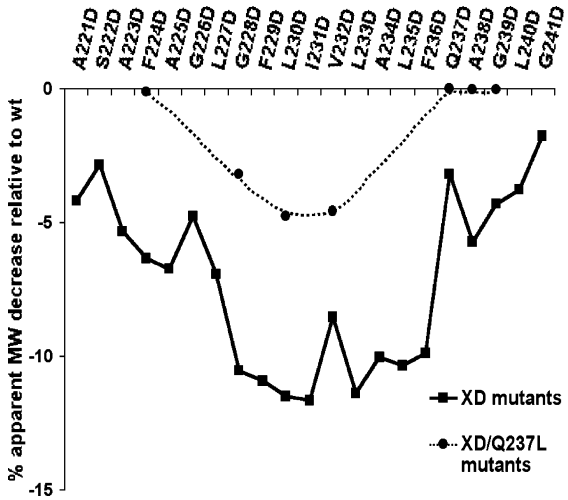

FIGURE 7: Comparative migration rates on SDS−PAGE gels for the CFTR TM4 D mutants (221−241), and corresponding selected XD/Q237L mutants. In each set, the points have been connected to indicate the trends involved, although the trend line for the seven XD/Q237L mutants is drawn arbitrarily and would not detect any extant periodicity. Each of the 21 XD/Q207L mutants (not shown on this graph) migrated as the wild-type (Figure 4). See the text for further discussion.

an assumption that must be regarded as tentative in view of the complex folding of TM domains revealed, for example, in crystallographic studies of the MsbA ABC transporter system from *E. coli* (*32*) and K^+ channel structures (*33*).

Involvement of Q237 in the H-Bond Network. To investigate the role of Q237 in TM4 among all the X → D mutants, Q237 was mutated to Leu, while the D mutants were retained at selected sites along the TM4 helix. From the results (Figures 5 and 7), we found that double mutants where D is relatively distant from Q207 in TM3 (F224D/Q237L, A238D/Q237L, and G239D/Q237L) returned to the wt migration rate, whereas the other double mutants (V232D/Q237L and L230D/Q237L) migrated more slowly than the corresponding D mutants, but still significantly faster than the wt construct. Thus, Q237 in TM4 becomes involved in the H-bond network, where it apparently helps to pull the two helices closer once the Q207 residue has stabilized the closed TM3/4 structure by partnering with a TM4 D residue. Therefore, without Q237 (i.e., with Q237 mutated to Leu), the X → D mutants in TM4 become more open through regions encompassing A221D to G228D, and Q237D to G241D, and are ultimately unable to form an H-bond with Q207. These results likely reflect the tendency of the TM3/4 system to utilize all available routes to energy minimization of the final structure.

The CF-phenotypic Mutant V232D Is Not the Optimal Position for Interhelix H-Bond Formation. As elaborated in Figure 3b, the CF-phenotypic mutant V232D does not form the tightest H-bond with Q207 in TM3 in comparison to the several X → D mutants on TM4. In fact, the migration rate of V232D is statistically slower vs those of D mutants at 229, 230, 231, and 233 (double asterisks, Figure 3b). In fact, the I231D construct has the greatest percentage molecular weight decrease relative to the wt, and ostensibly forms the tightest H-bond with Q207 (illustrated with energy-minimized helical dimers in Figure 6). As V232D is the CF-phenotypic mutant in this series, this result initially appeared counterintuitive. It should be noted, however, that Ile requires two base changes in codon to mutate to Asp, which is extremely less probable in nature (*11*). Nevertheless, for any A → D or G → D mutants (in this case, A221D, A223D, G226D, G228D, A234D, A238D, G239D, and G241D), only a single-base change is required, and therefore, it is possible these mutants represent potential phenotypic CF mutants, which have yet to be discovered. It is also interesting to note that several mutants—including S222D, G226D, V232D, and Q237D—display locally slower migration rates. While these positions correlate only irregularly to the "periodicity" of the TM4 helix (solid line, Figure 7), this result suggests the possibility that residues nominally oriented on an outward rather than an interfacial position in TM3/4 (Figure 6b) may require the greatest rotational reorientation to participate with the TM3 partner. One might speculate that this is the case for CF-phenotypic mutant V232D, and therefore, its capture by Q207 necessitates major reorientation of the wild-type TM4 axis—and accordingly the greatest disruption of the native folded domain structure. These circumstances, in conjunction with our finding that the Q207 "capture radius" can extend 2−3 turns of the TM4 in either direction from a presumed mid-TM3 helix position of Q207, may have important implications for the structural consequences of disease-causing mutations in membrane proteins.

REFERENCES

1. Grigorieff, N., Ceska, T. A., Downing, K. H., Baldwin, J. M., and Henderson, R. (1996) Electron-crystallographic refinement of the structure of bacteriorhodopsin, *J. Mol. Biol. 259*, 393−421.
2. Zhou, F. X., Cocco, M. J., Russ, W. P., Brunger, A. T., and Engelman, D. M. (2000) Interhelical hydrogen bonding drives strong interactions in membrane proteins, *Nat. Struct. Biol. 7* (2), 154−160.
3. Choma, C., Gratkowski, H., Lear, J. D., and DeGrado, W. F. (2002) Asparagine-mediated self-association of a model transmembrane helix, *Nat. Struct. Biol. 7* (2), 161−166.
4. Stevens, T. J., and Arkin, I. T. (1999) Are membrane proteins "inside-out" proteins, *Proteins 36* (1), 135−143.
5. Cary, J. M., and Moore, J. S. (2002) Hydrogen bond-stabilized helix formation of a *m*-phenylene ethynylene oligomer, *Org. Lett. 4* (26), 4663−4666.
6. Adamian, L., and Liang, J. (2002) Interhelical hydrogen bonds and spatial motifs in membrane proteins: polar clamps and serine zippers, *Proteins 47*, 209−218.
7. Cary, J. M., and Moore, J. S. (2002) Hydrogen bond-stabilized helix formation of a *m*-phenylene ethynylene oligomer, *Org. Lett. 4* (26), 4663−4666.
8. Pogozheva, I. D., Lomize, A. L., and Mosberg, H. I. (1998) Opioid receptor three-dimensional structures from distance geometry calculations with hydrogen bonding constraints, *Biophys. J. 75* (2), 612−634.
9. Shrivastava, I. H., Capener, C. E., Forrest, L. R., and Sansom, M. S. P. (2002) Structure and dynamics of K channel pore-lining helices: a comparative simulation study, *Biophys. J. 78* (1), 79−92.
10. Partridge, A. W., Therien, A. G., and Deber, C. M. (2002) Polar mutations in membrane proteins as a biophysical basis for disease, *Biopolymers 66* (5), 350−358.
11. Partridge, A. W., Therien A. G., and Deber, C. M. (2004) Missense mutations in transmembrane domains of proteins: phenotypic propensity of polar residues for human disease, *Proteins 54* (4), 648−656.
12. Riordan, J. R., Rommens, J. M., Kerem, B., Alon, N., Rozmahel, R., Grzelczak, Z., Zielenski, J., Lok, S., Plavsic, N., Chou, J. L., and et al. (1989) Identification of the cystic fibrosis gene: cloning and characterization of complementary DNA, *Science 245*, 1066−1073.
13. Akabas, M. H., Cheung, M., and Guinamard, R. (1997) Probing the structural and functional domains of the CFTR chloride channel, *J. Bioenerg. Biomembr. 29*, 453−463.

14. Akabas, M. H. (2000) Cystic fibrosis transmembrane conductance regulator. Structure and function of an epithelial chloride channel, *J. Biol. Chem. 275*, 3729−3732.
15. Tan, A. L., Ong, S. A., and Venkatesh, B. (2002) Biochemical implications of sequence comparisons of the cystic fibrosis transmembrane conductance regulator, *Arch. Biochem. Biophys. 401*, 215−222.
16. Gong, X., Burbridge, S. M., Cowley, E. A., and Linsdell, P. (2002) Molecular determinants of Au(CN)(2)(−) binding and permeability within the cystic fibrosis transmembrane conductance regulator Cl(−) channel pore, *J. Physiol. 540*, 39−47.
17. Chen, J. M., Cutler, C., Jacques, C., Boeuf, G., Denamur, E., Lecointre, G., Mercier, B., Cramb, G., and Ferec, C. (2001) A combined analysis of the cystic fibrosis transmembrane conductance regulator: implications for structure and disease models, *Mol. Biol. Evol. 18*, 1771−1788.
18. Peng, S., Liu, L. P., Emili, A. Q., and Deber, C. M. (1998) Cystic fibrosis transmembrane conductance regulator: expression and helicity of a double membrane-spanning segment, *FEBS Lett. 431*, 29−33.
19. Linsdell, P. (2001) Relationship between anion binding and anion permeability revealed by mutagenesis within the cystic fibrosis transmembrane conductance regulator chloride channel pore, *J. Physiol. 531*, 51−66.
20. Linsdell, P., and Gong, X. (2002) Multiple inhibitory effects of Au(CN)(2-) ions on cystic fibrosis transmembrane conductance regulator Cl(−) channel currents, *J. Physiol. 540*, 29−38.
21. Cystic Fibrosis Genetic Analysis Consortium, http://www.genet.sickkids.on.ca/cgi-bin/WebObjects/MUTATION.
22. Therien, A. G., Grant, F. E., and Deber, C. M. (2001) Interhelical hydrogen bonds in the CFTR membrane domain, *Nat. Struct. Biol. 8*, 597−601.
23. White, S. H., and Wimley, W. C. (1999) MEMBRANE PROTEIN FOLDING AND STABILITY: Physical Principles, *Annu. Rev. Biophys. Biomol. Struct. 28*, 319−365.
24. Therien, A. G., Glibowicka, M., and Deber, C. M. (2002) Expression and purification of two hydrophobic double-spanning membrane proteins derived from the cystic fibrosis transmembrane conductance regulator, *Protein Expr. Purif. 25* (1), 81−86.
25. Partridge, A. W., Melnyk, R. A., and Deber, C. M. (2002) Polar residues in membrane domains of proteins: molecular basis for helix-helix association in a mutant CFTR transmembrane segment, *Biochemistry 41*, 3647−3653.
26. Chu, D. M., Francis, S. H., Thomas, J. W., Maksymovitch, E. A., Fosler, M., and Corbin, J. D. (1998) Activation by autophosphorylation or cGMP binding produces a similar apparent conformational change in cGMP-dependent protein kinase, *J. Biol. Chem. 273*, 14649−14656.
27. Otsuka, F., Okugaito, I., Ohsawa, M., Iwamatsu, A., Suzuki, K., and Koizumi, S. (2000) Novel responses of ZRF, a variant of human MTF-1, to in vivo treatment with heavy metals, *Biochem. Biophys. Acta 1492*, 330−340.
28. Wang, C., and Deber, C. M. (2000) Peptide mimics of the M13 coat protein transmembrane segment. Retention of helix-helix interaction motifs, *J. Biol. Chem. 275*, 16155−16159.
29. Adams, P. D., Arkin, I. T., Engelman, D. M., and Brünger, A. T. (1995) Computational searching and mutagenesis suggest a structure for the pentameric transmembrane domain of phospholamban, *Nat. Struct. Biol. 2*, 154−162.
30. Baker, E. N., and Hubbard, R. E. (1984) Hydrogen bonding in globular proteins, *Prog. Biophys. Mol. Biol. 44*, 97−179.
31. Faham, S., Yang, D., Bare, E., Yohannan, J., Whitelegge, J. P., and Bowie, J. U. (2004) Side-chain contributions to membrane protein structure and stability, *J. Mol. Biol. 335*, 297−305.
32. Chang, G., and Roth, C. B. (2001) Structure of MsbA from E. coli: a homolog of the multidrug resistance ATP binding cassette (ABC) transporters, *Science 293* (5536), 1793−800.
33. MacKinnon, R. (2003) Potassium channel, *FEBS Lett. 555* (1), 62−65.
34. Popot, J. L., and Engelman, D. M. (2000) Helical membrane protein folding, stability, and evolution, *Annu. Rev. Biochem. 69*, 881−922.
35. Deber, C. M., and Goto, N. K. (1996) Folding proteins into membranes, *Nat. Struct. Biol. 3* (10), 815−818.
36. Baker, E. N., and Hubbard, R. E. (1984) Hydrogen bonding in globular proteins, *Prog. Biophys. Mol. Biol. 44*, 97−179.

BI0494525